JOURNAL of the TURKISH CHEMICAL SOCIETY
SECTION: B
CHEMICAL ENGINEERING
TURKISH CHEMICAL SOCIETY

The Production and Characterization of Activated Carbon Using Pistachio Shell through Carbonization and CO_2 Activation

İlhan Küçük[a], Yunus Önal[b*], Canan Akmil-Başar[b]

[a] Department of Chemistry, Faculty of Art and Science, Inonu University, 44280 Malatya, Turkey
[b] Department of Chemical Engineering, Faculty of Engineering, Inonu University, 44280 Malatya, Turkey

Abstract: In this study, activated carbon from pistachio shell has been successfully produced through carbonization and CO_2 activation. The pistachio shell has been carbonized at 300, 400, 500, 600, 700, 800, 900, and 1000 °C temperature, and 100 and 500 mL / min inert nitrogen atmosphere. Char, liquid and gas yields have been investigated during the carbonization process. In the carbonization, generally the solid yield decreases as the temperature increases, while the gas efficiency increases. The increase in liquid yield was lower than the gas yield. Carbonized samples were subjected to physical activation with carbon dioxide at a flow rate of 100 mL / min at 800 °C and 900 °C. As a result of carbon dioxide activation, BET surface area values were obtained in the range of 16.66-857.13 m^2 / g. The highest surface area was obtained as 857.13 m^2 / g. at 600 °C carbonization temperature, 100 mL / min nitrogen flow rate and 800 °C activation temperature 100 mL / min carbon dioxide flow rate. The mean pore diameter values of the activated carbon samples were measured in the range of 2.07-4.06 nm. The average pore size distribution of some of the samples is in a relatively narrow range and is mostly of molecular sieve size in nano pore size. According to the XRD results, all samples were found to be amorphous.

Keywords: Biomass, carbonization, physical activation, activated carbon.

Submitted: November 07, 2018. **Accepted:** February 28, 2019.

Cite this: Küçük İ, Önal Y, Akmil-Başar C. The Production and Characterization of Activated Carbon Using Pistachio Shell through Carbonization and CO2 Activation. JOTCSB. 2019;2(1): 35–44.

***Corresponding author. E-mail:** yunus.onal@inonu.edu.tr.

INTRODUCTION

Increasing industrialization brings the population to cities and as a result, it brings water and air pollution to a great extent. Due to the increase in the consumption of metropolises, the diversity of pollutants is greatly increasing. As a result of this increase, especially the contamination concentrations of the aqueous media are large. Pollution is in domestic and industrial wastewater, thrown into the environment by mixing with rain and snow water from the soil. Therefore, the treatment of water in the treatment plants alone cannot solve the pollution problem. The concentration of pollutants, especially drugs used for humans and animals, increases rapidly. Apart from this, in order to meet the increasing food needs of people, the use of pesticides as a result of agriculture is also an important pollution. The chemicals that are mixed in the soil, pollute the ground water from here and the underground waters reach the lakes and seas by the streams. The pesticide and herbicides used are halogen-derived and the capacity to form a large number of new compounds in the natural environment increases the pollution (1).

In addition to this pollution, air pollution, which is another problem of the increasing world population, is also important for years. In particular, the growth of cities and the advancement of industry have significantly increased air pollution. This pollution affects human life and affects many life forms and makes the world uninhabitable. At this point, air pollution should be considered besides water pollution (1, 2).

Adsorption is an important process widely used in both water and air pollution removal. Thanks to this process, the polluted water has been cleaned and re-used for many years, even the existing swamps and the water communities that cannot be used are reintroduced as drinking water. Activated carbon has an important role in the adsorbents used for this purpose. Activated carbon is the most widely used in adsorbents due to its micro and meso pore structure with high surface area (1, 2). Activated carbon is generally derived from coal and biomass and in recent years it has been started to be obtained from waste polymers. The variety and amount of biomass has become important in the production of activated carbon. The need for annual global activated carbon needs of 3 million tons and a 7% growth each year led to the increase in raw material diversity and even the use of all carbon containing waste for this purpose. As a result, both waste materials will be freed and these substances will be evaluated and re-used. In addition, the synthesis methods developed by these sources are gaining importance in increasing both surface areas and pore sizes of the adsorbents obtained from these sources. Agricultural wastes, especially found in our country, are very suitable for active carbon synthesis (3-11). The reason for this is the high amount of agricultural waste used as raw material and the carbon content of these wastes is suitable for the production of activated carbon (12-14).

Chemical and physical activation methods are generally used in the production of activated carbon (15, 16). In the physical activation, the carbonization process of the raw materials in different temperature ranges is found in the literature (17-19). The liquid and gas released during the process are used directly in the production of energy (20). The carbonized samples may be subjected to activation at different temperatures using steam and / or carbon dioxide. Changes in surface area can be seen depending on the activation method used (21-23).

In this study, biomass pistachio shell was used as the raw material. Activation of carbon dioxide was carried out after carbonization and activated carbon was produced as molecular sieve. In the carbonization process, pyrolysis gas yield, condensable pyrolysis oil yield and solid (char) yield were calculated. The activated carbon yield was calculated after activation. Surface area of activated carbon, FTIR, XRD, SEM characterization was evaluated.

EXPERIMENTAL AND THEORETICAL STUDIES

100 kg of pistachio shell was taken without taking any action (original moisture weight 4.97 %) and it was used in the experiments. Carbonization was carried out using a cylindrical furnace with a temperature adjustment of three zones. The steel reactor has an internal diameter of 8.2 cm and is suitable for gas inlet and condensable liquid outlet. A liquid fraction was collected which could be condensed by attaching two coolers to the reactor outlet. Activation was performed in a separate three-zone cylindrical furnace in quartz glass tube (inner diameter: 4 cm).

Surface area measurements of activated carbon samples were made by the Micromeritics TriStar 3000 surface analyzer. The surface area was determined from isotherm using the BET method (S_{BET}). Ash determination was made according to ASTM D2866-11 standard at 650°C. XRD measurements were made in Japanese Rigaku RadB-DMAX II (Cu K-alpha) system.

RESULTS AND DISCUSSION

Solid (char), liquid and gas yield results of carbonization samples is given in the Table 1.

Table 1: Solid (char), liquid and gas yield results of carbonized samples.

Temperature	N_2 Flowrate	Char Yield %	Liquid Yield %	Gas Yield %
300 °C	100 mL / min	40.89	37.85	21.26
400 °C	100 mL / min	29.63	43.94	26.43
500 °C	100 mL / min	25.69	43.11	31.20
600 °C	100 mL / min	24.05	48.04	27.91
700 °C	100 mL / min	23.10	39.85	37.05
800 °C	100 mL / min	23.30	36.90	39.80
900 °C	100 mL / min	23.67	40.67	35.66
1000 °C	100 mL / min	23.36	37.89	38.75
1000 °C	500 mL / min	22.77	36.83	40.40

As the temperature changes, the solid and liquid yield was varied. While this change is generally in the decrease in solid yield, decreases and increases in gas and liquid yield were observed. This situation can be explained by the deformation of the macromolecular structure with the effect of temperature. In addition, at high temperature (900 °C and above), the efficiency of the liquid decreases while the efficiency of the gas increases. Small groups are separated from the macromolecular structure at high temperature and passed to the gas phase. This reduces the liquid yield and increases the gas efficiency (24-26).

Table 2: BET analysis results of samples.

Carbonization		Physical Activation								
Temperature °C	N_2 Flowrate (mL/min)	Temperature °C (100 mL/min CO_2)	S_{BET} m^2/g	S_{micro} m^2/g	S_{meso} m^2/g	V_T cm^3/g	V_{micro} cm^3/g	V_{meso} cm^3/g	dp^a nm
300	100	800	394.64	343.44	51.20	0.21	0.18	0.03	2.20
300	100	900	530.57	439.81	90.76	0.28	0.23	0.05	2.18
400	100	800	401.71	365.00	36.71	0.21	0.19	0.02	2.15
500	100	800	759.74	12.76	746.98	0.75	0.04	0.71	4.06
600	100	800	857.13	788.98	68.14	0.41	0.09	0.32	2.07
700	100	900	473.93	413.38	60.55	0.24	0.21	0.03	2.04
800	100	900	518.70	448.55	70.15	0.27	0.23	0.04	2.13
900	100	800	179.62	179.62	-	-	0.15	-	-
1000	500	800	16.66	16.66	-	-	0.04	-	-
1000	500	900	295.40	295.40	-	-	0.18	-	-

S: Surface area, V: volume dp: average pore diameter a: (4 V/A by BET)

When the results in Table 2 were examined, the total pore volume (V_T) was low at the low carbonization temperature while the micro pore surface area (S_{micro}) was maximum. The highest surface area was obtained for the sample synthesized at an activation temperature of 800 ºC and a carbonization temperature of 600 ºC. The micro pore surface area of the sample covers 92.04% of the total area. The average pore diameter is 2.04 nm and the pore size distribution is very narrow. As a result, carbonization and subsequent activation of carbon dioxide yielded molecular sieve activated carbon with nano-pore. DFT (Density Functional Theory) measurements of some activated carbons were obtained and as a result of these measurements, the presence of micropores in the structure was proven. The majority of the pore size are between 1-2 nanometers. The some sample of pore size distribution graph is given in Figure 1. Figure 2 shows the typical adsorption isotherm of N_2

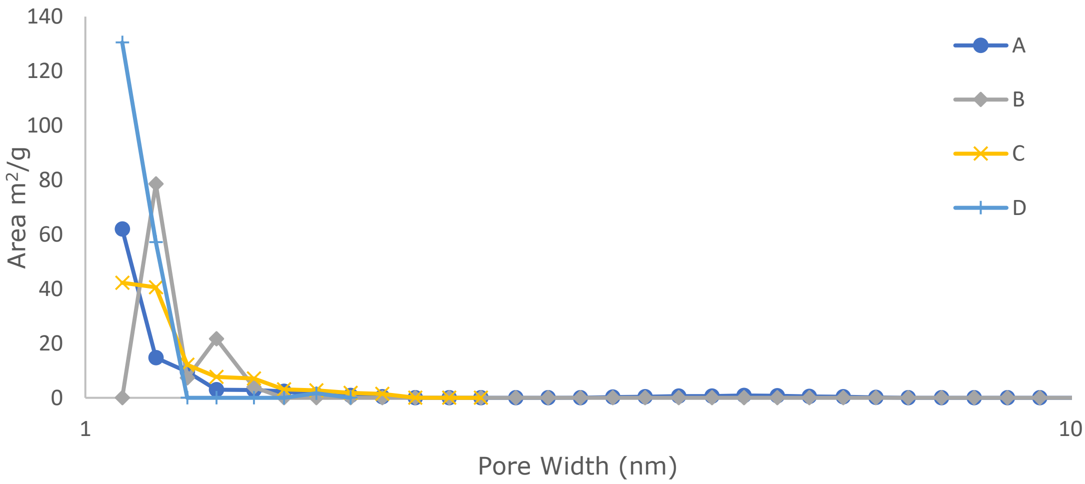

Figure 1: Pore size distribution of activated carbon sample **A.** at 300 °C 100 ml / min N_2 carbonization and at 800°C with 100 mL / min CO_2 activation **B.** at 600 °C 100 mL / min N_2 carbonization and at 800 °C with 100 mL / min CO_2 activation. **C.** at 800 °C 100 mL / min N_2 carbonization and at 900 °C with 100 mL / min CO_2 activation, **D.** at 900 °C 100 mL / min N_2 carbonization and at 800 °C with 100 mL / min CO_2 activation.

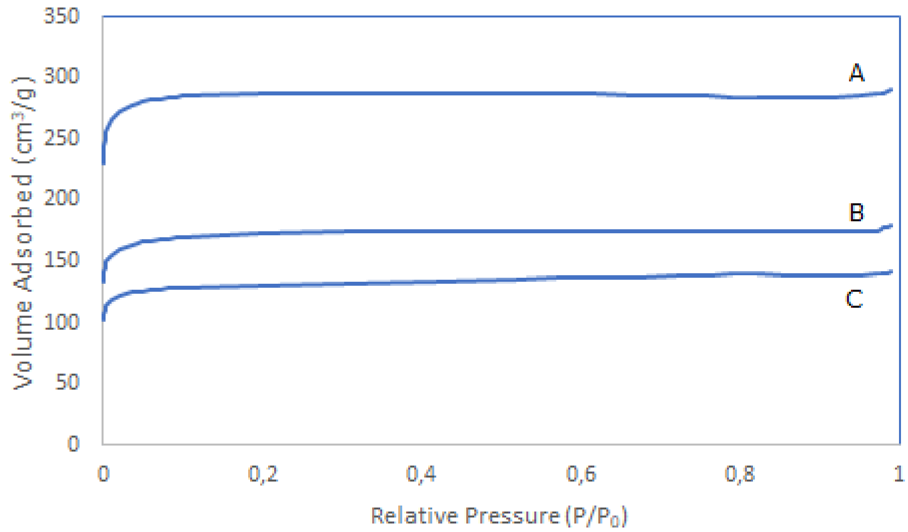

Figure 2: Adsorption isotherms of N_2 **A**. Activated carbon sample at 600 °C 100 mL / min N_2 carbonization and at 800°C with 100 mL / min CO_2 activation **B.** Activated carbon sample at 800 °C 100 mL / min N_2 carbonization and at 900 °C with 100 mL / min CO_2 activation. **C**. Activated carbon sample at 300 °C 100 mL / min N_2 carbonization and at 800 °C with 100 mL / min CO_2 activation.

When the adsorption isotherms were taken into consideration, it was determined that the samples obtained corresponded to the Type 1 isotherm (27-29). The general feature of the Type I isotherm is that it contains large amounts of micropores in the structure of the adsorbent. At low P / Po values, adsorption increased and then isotherm were on a flat plateau. As the P / Po value increases, the increase in adsorption is explained by the regularity of the pore size distribution (30-32).

Figure 3 shows the FTIR spectrum of raw material and activated carbon samples. FTIR spectra seen around 3600 cm^{-1} seen from the peak cellulosic structure belong to O-H groups. As a result of the structural arrangement resulting from the heat treatment, the hydroxyl groups were greatly reduced. The peaks at about 2900 cm^{-1} indicate the aliphatic C-H strength. These peaks are increased by the introduction of the raw material into the structural arrangement. The increase of aliphatic strength peaks with the increase in temperature is another proof of structural regulation. In addition, multiple peaks at this wavelength result from the vibration of the methylene groups. Similarly, peaks at this wavelength result from the vibration of peaks such as $-CH_3$, $-CH_2CH_3$ and $-CH_2$. The peaks at approximately 1000 cm^{-1} show that there is a C-C bond in the structure (33-35). When these results were taken into consideration, it was seen that the structure was similar to each other.

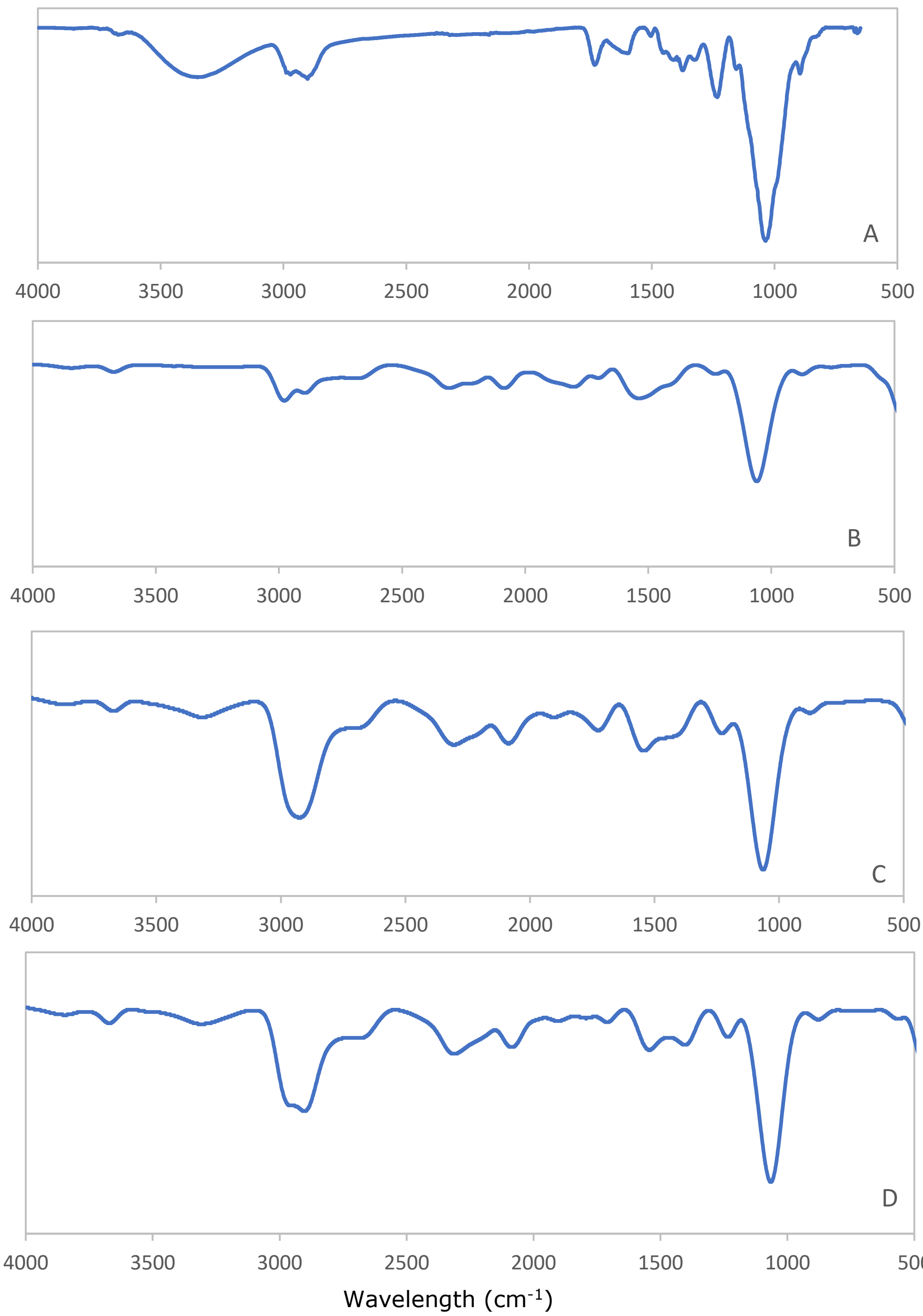

Figure 3: FTIR spectrum of raw material and activated carbon samples. **A.** Raw Pistachio Shell **B.** Activated carbon sample at 500 °C 100 mL / min N_2 carbonization and at 800°C with 100 mL / min CO_2 activation **C.** Activated carbon sample at 600 °C 100 mL / min N_2 carbonization and at 800 °C with 100 mL / min CO_2 activation **D.** Activated carbon sample at 1000 °C 500 mL / min N_2 carbonization and at 900 °C with 100 mL / min CO_2 activation.

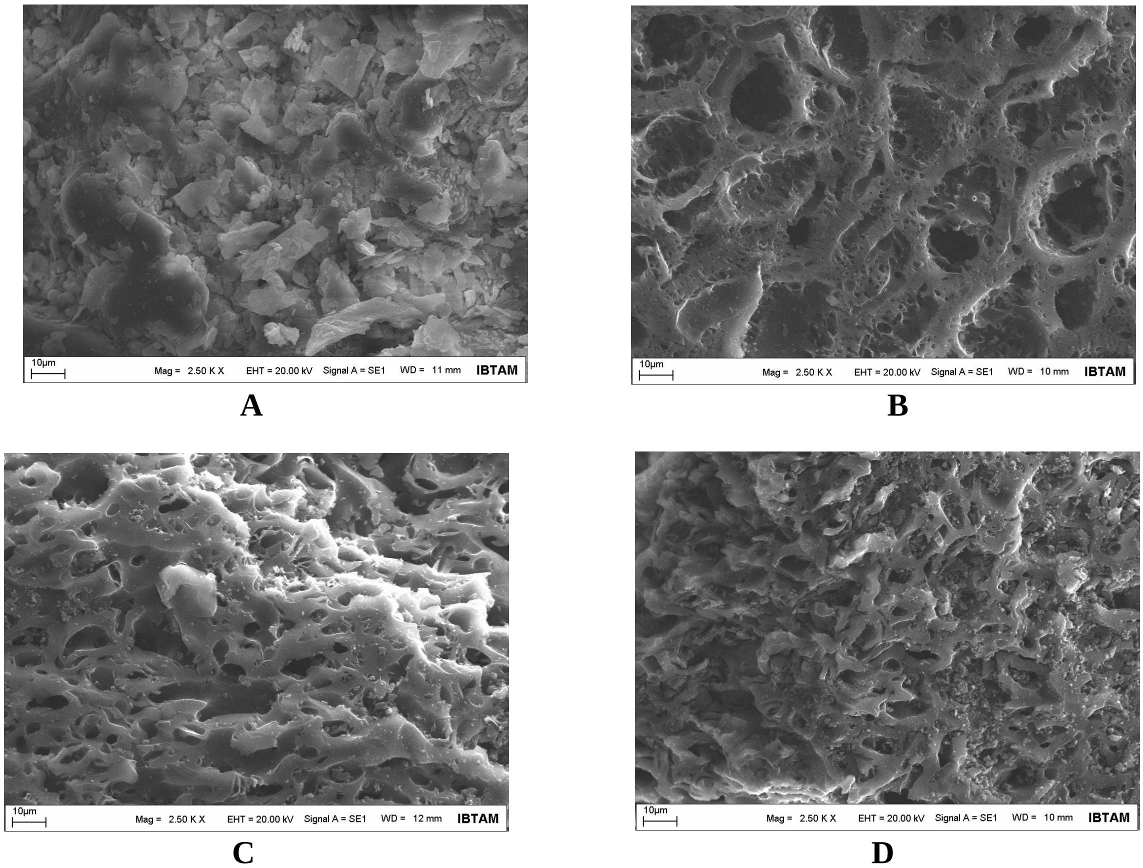

Figure 4: **A.** SEM image of raw pistachio shell **B.** Activated carbon sample at 600 °C 100 ml / min N_2 carbonization and at 800 °C with 100 mL / min CO_2 activation **C** Activated carbon sample at 500 °C 100 mL / min N_2 carbonization and at 800 °C with 100 mL / min CO_2 activation **D.** Activated carbon sample at 300 °C 100 mL / min N_2 carbonization and at 800 °C with 100 mL / min CO_2 activation.

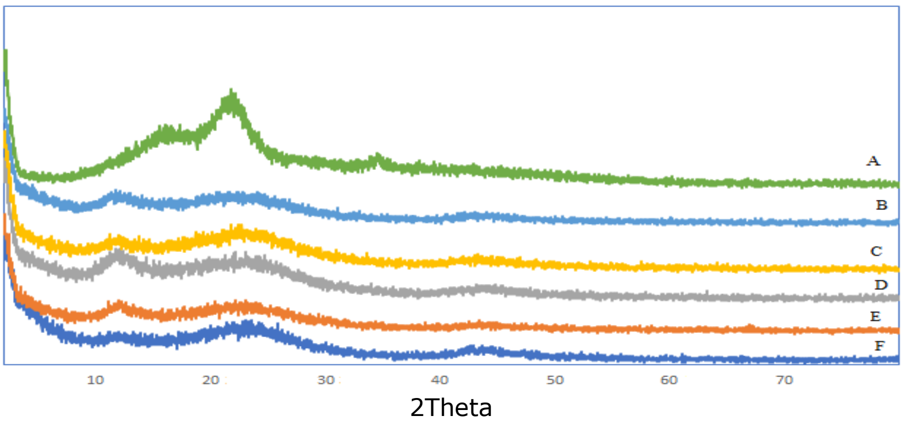

Figure 5: XRD chart of samples **A.** XRD chart of raw pistachio shell **B.** Activated carbon sample at 400 °C 100 mL / min N_2 carbonization and at 800 °C with 100 mL / min CO_2 activation **C.** Activated carbon sample at 500 °C 100 mL / min N_2 carbonization and at 800 °C with 100 mL / min CO_2 activation i **D.** Activated carbon sample at 600 °C 100 mL / min N_2 carbonization and at 800 °C with 100 mL / min CO_2 activation **E.** Activated carbon sample at 900 °C 100 mL / min N_2 carbonization and at 800 °C with 100 mL / min CO_2 activation **F.** Activated carbon sample at 1000 °C 500 mL / min N_2 carbonization and at 900 °C with 100 mL / min CO_2 activation.

In the SEM images shown in Figure 4, no visible pores are present in the pistachio shell used as raw material. But carbonization and physical activation result in the formation of pores. With the increase in temperature, it is seen that pores appear as a result of the separation of small organic groups within the macromolecular structure. In the original macromolecular structure of pistachio, it is concluded that the pores have the same size as the molecular units are composed of structures of similar size. The homogeneity of the pores shows that the activated carbon is in the form of a molecular sieve.

Figure 5 shows the XRD graphs of raw materials and activated carbon samples. As can be understood from the XRD plot of raw pistachio, the structure is largely amorphous. 3 different amorphous structures in the structure can be expressed as macromolecular groups. Crystalline units are separated from the structure with the effect of temperature and the structure turns into completely amorphous structure. As in the original raw sample, three different macromolecular main units remain in the structure (36, 37).Table 3 shows the ash values of samples

Table 3: Ash values of samples.

Carbonization		Physical Activation	
Temperature (°C)	N_2 Flow rate (mL/min)	Temperature (°C) Gas Flow rate (100 mL/min CO_2)	Ash %
	Raw pistachio shell		0.380
300	100	800	0.020
300	100	900	0.019
400	100	800	0.017
500	100	800	0.019
600	100	800	0.019
700	100	900	0.018
800	100	900	0.024
900	100	800	0.028
1000	500	800	0.020
1000	500	900	0.025

When the ash values of the samples are examined, the ash value of the raw materials is high but the ash values of the synthesized materials are lower than the raw materials. It can be explained by the fact that the inorganic components forming the ash in the structural arrangement are inorganic elements degraded at high temperature and also they are in organic chelate structure. Low temperature ash can be explained by the chelate structure. At high temperature, the mass increased due to the loss of organic structure. The elemental analysis results of samples is given in Table 4.

Table 4: Elemental analysis results of samples.

Samples		%C	%H	%N	%S	%O*
Raw Pistachio Shell		47.37	5.896	-	-	46.734
300 °C	100 mL/min N_2 800°C CO_2	58.39	1.102	-	-	40.508
300 °C	100 mL/min N_2 900°C CO_2	88.98	0.717	-	-	10.303
400 °C	100 mL/min N_2 800°C CO_2	65.61	1.157	0.144	-	33.089
500 °C	100 mL/min N_2 800°C CO_2	89.84	1.109	-	-	9.051
600 °C	100 mL/min N_2 800°C CO_2	86.57	1.131	-	-	12.299
700 °C	100 mL/min N_2 800°C CO_2	87.11	1.049	0.124	-	11.717
900 °C	100 mL/min N_2 800°C CO_2	64.49	0.803	0.308	-	34.399
1000 °C	500 mL/min N_2 800°C CO_2	58.07	0.789	0.599	-	40.542
1000 °C	500 mL/min N_2 900°C CO_2	68.85	0.658	0.348	-	30.144

* *Calculated by difference*

Considering the results of the elemental analysis, it was observed that the percentage of carbon in the synthesized materials increased as compared to the raw material. In addition, there is a decrease in the amounts of hydrogen and oxygen. The decrease in their amounts indicates structural regulation. Methylene blue adsorption capacity of samples is in Table 5.

.

Table 5: Methylene blue adsorption capacity of samples.

Carbonization		Physical Activation		
Temperature (°C)	N_2 Flow rate (mL/min)	Temperature (°C) Gas Flow rate (100 mL/min CO_2)	S_{BET} m^2/g	Adsorption Capacity q_e (mg/g)
300	100	800	394.64	25.31
300	100	900	530.57	93.45
400	100	800	401.71	19.48
600	100	800	857.13	5.95
700	100	900	473.93	68.54
800	100	900	518.70	91.16
900	100	800	179.62	32.79
1000	500	800	16.66	1.77
1000	500	900	295.40	19.59

Methylene blue adsorption on samples was studied. 0.1 gram of active carbon samples were taken into 100 mL 100 ppm methylene blue solution and samples were measured after 24 hours. In the results, the adsorption capacity of methylene blue was calculated and given as a table. As seen in the BET measurements and DFT measurements, the working samples have the majority of micro pores and their adsorption capacity is low. Methylene blue is a compound with a molecule size of approximately 1.43 nm (38, 39) and methylene blue molecules do not enter the pore (40). Therefore, their adsorption capacity is low.

ACKNOWLEDGEMENT

This study was supported by the unit of Scientific Researches of Inonu University in Malatya, Turkey; Project no: FDI-2017-680

REFERENCES

1. Dias JM, Alvim-Ferraz MC, Almeida MF, Rivera-Utrilla J, Sánchez-Polo M. Waste materials for activated carbon preparation and its use in aqueous-phase treatment: a review. Journal of environmental management. 2007;85(4):833–846.

2. Rafatullah M, Sulaiman O, Hashim R, Ahmad A. Adsorption of methylene blue on low-cost adsorbents: a review. Journal of hazardous materials. 2010;177(1–3):70–80.

3. Yagmur E, Ozmak M, Aktas Z. A novel method for production of activated carbon from waste tea by chemical activation with microwave energy. Fuel. 2008 Nov;87(15–16):3278–85.

4. Özdemir M, Bolgaz T, Saka C, Şahin Ö. Preparation and characterization of activated carbon from cotton stalks in a two-stage process. Journal of Analytical and Applied Pyrolysis. 2011;92(1):171–175.

5. Şahin Ö, Saka C. Preparation and characterization of activated carbon from acorn shell by physical activation with H2O–CO2 in two-step pretreatment. Bioresource technology. 2013;136:163–168.

6. Dolas H, Sahin O, Saka C, Demir H. A new method on producing high surface area activated carbon: The effect of salt on the surface area and the pore size distribution of activated carbon prepared from pistachio shell. Chemical engineering journal. 2011;166(1):191–197.

7. Gonzalez JF, Roman S, González-García CM, Nabais JV, Ortiz AL. Porosity development in activated carbons prepared from walnut shells by carbon dioxide or steam activation. Industrial & engineering chemistry research. 2009;48(16):7474–7481.

8. Kütahyalı C, Eral M. Sorption studies of uranium and thorium on activated carbon prepared from olive stones: kinetic and thermodynamic aspects. Journal of Nuclear Materials. 2010;396(2–3):251–256.

9. Şayan E. Ultrasound-assisted preparation of activated carbon from alkaline impregnated hazelnut shell: An optimization study on removal of Cu2+ from aqueous solution. Chemical Engineering Journal. 2006;115(3):213–218.

10. Georgin J, Dotto GL, Mazutti MA, Foletto EL. Preparation of activated carbon from peanut shell by conventional pyrolysis and microwave irradiation-pyrolysis to remove organic dyes from aqueous solutions. Journal of Environmental Chemical Engineering. 2016;4(1):266–275.

11. Depci T, Onal Y, Prisbrey KA. Apricot stone activated carbons adsorption of cyanide as revealed from computational chemistry analysis and experimental study. Journal of the Taiwan Institute of Chemical Engineers. 2014 Sep;45(5):2511–7.

12. Kadirvelu K, Kavipriya M, Karthika C, Radhika M, Vennilamani N, Pattabhi S. Utilization of various agricultural wastes for activated carbon preparation and application for the removal of dyes and metal ions from aqueous solutions. Bioresource Technology. 2003 Mar;87(1):129–32.

13. Ioannidou O, Zabaniotou A. Agricultural residues as precursors for activated carbon production—A review. Renewable and Sustainable Energy Reviews. 2007 Dec;11(9):1966–2005.

14. Yahya MA, Al-Qodah Z, Ngah CWZ. Agricultural bio-waste materials as potential sustainable precursors used for activated carbon production: A review.

Renewable and Sustainable Energy Reviews. 2015 Jun;46:218–35.

15. Kilic M, Apaydin-Varol E, Pütün AE. Adsorptive removal of phenol from aqueous solutions on activated carbon prepared from tobacco residues: Equilibrium, kinetics and thermodynamics. Journal of Hazardous Materials. 2011 May;189(1–2):397–403.

16. Rodríguez-Reinoso F, Molina-Sabio M. Activated carbons from lignocellulosic materials by chemical and/or physical activation: an overview. Carbon. 1992;30(7):1111–8.

17. Bouchelta C, Medjram MS, Bertrand O, Bellat J-P. Preparation and characterization of activated carbon from date stones by physical activation with steam. Journal of Analytical and Applied Pyrolysis. 2008 May;82(1):70–7.

18. Thommes M. Physical Adsorption Characterization of Nanoporous Materials. Chemie Ingenieur Technik. 2010 Jun 14;82(7):1059–73.

19. Yun CH, Park YH, Park CR. Effects of pre-carbonization on porosity development of activated carbons from rice straw. Carbon. 2001 Apr;39(4):559–67.

20. Lee H, Kim Y-M, Kim S, Ryu C, Park S, Park Y-K. Review of the use of activated biochar for energyand environmental applications. Carbon Lett. 2018;26:1–10.

21. Marsh H, Rodríguez-Reinoso F. Activated carbon. 1st ed. Amsterdam ; Boston: Elsevier; 2006. 536 p.

22. Ahmadpour A, Do DD. The preparation of activated carbon from macadamia nutshell by chemical activation. Carbon. 1997;35(12):1723–32.

23. Pallarés J, González-Cencerrado A, Arauzo I. Production and characterization of activated carbon from barley straw by physical activation with carbon dioxide and steam. Biomass and Bioenergy. 2018 Aug;115:64–73.

24. Giudicianni P, Cardone G, Ragucci R. Cellulose, hemicellulose and lignin slow steam pyrolysis: Thermal decomposition of biomass components mixtures. Journal of Analytical and Applied Pyrolysis. 2013 Mar;100:213–22.

25. Burhenne L, Messmer J, Aicher T, Laborie M-P. The effect of the biomass components lignin, cellulose and hemicellulose on TGA and fixed bed pyrolysis. Journal of Analytical and Applied Pyrolysis. 2013 May;101:177–84.

26. Cabrales L, Abidi N. On the thermal degradation of cellulose in cotton fibers. Journal of Thermal Analysis and Calorimetry. 2010 Nov;102(2):485–91.

27. Rouquerol F, Rouquerol J, Sing KSW, Llewellyn PL, Maurin G. Adsorption by powders and porous solids: principles, methodology and applications. Second edition. Amsterdam: Elsevier/AP; 2014. 626 p.

28. Labani MM, Rezaee R, Saeedi A, Hinai AA. Evaluation of pore size spectrum of gas shale reservoirs using low pressure nitrogen adsorption, gas expansion and mercury porosimetry: A case study from the Perth and Canning Basins, Western Australia. Journal of Petroleum Science and Engineering. 2013 Dec;112:7–16.

29. Collet F, Bart M, Serres L, Miriel J. Porous structure and water vapour sorption of hemp-based materials. Construction and Building Materials. 2008 Jun;22(6):1271–80.

30. Saka C. BET, TG–DTG, FT-IR, SEM, iodine number analysis and preparation of activated carbon from acorn shell by chemical activation with ZnCl2. Journal of Analytical and Applied Pyrolysis. 2012 May;95:21–4.

31. Bansal RC, Goyal M. Activated carbon adsorption [Internet]. Boca Raton: Taylor & Francis; 2005 [cited 2019 Mar 23]. Available from: http://www.crcnetbase.com/isbn/9780824753443

32. Ahmedna M, Marshall W., Rao R. Production of granular activated carbons from select agricultural by-products and evaluation of their physical, chemical and adsorption properties1Louisiana Agricultural Experiment Station manuscript 99-21-0066.1. Bioresource Technology. 2000 Jan;71(2):113–23.

33. Zhang Z, Xu M, Wang H, Li Z. Enhancement of CO2 adsorption on high surface area activated carbon modified by N2, H2 and ammonia. Chemical Engineering Journal. 2010 Jun;160(2):571–7.

34. Lua AC, Guo J. Microporous Oil-Palm-Shell Activated Carbon Prepared by Physical Activation for Gas-Phase Adsorption. Langmuir. 2001 Oct;17(22):7112–7.

35. Nabais JMV, Nunes P, Carrott PJM, Ribeiro Carrott MML, García AM, Díaz-Díez MA. Production of activated carbons from coffee endocarp by CO2 and steam activation. Fuel Processing Technology. 2008 Mar;89(3):262–8.

36. Okada K, Yamamoto N, Kameshima Y, Yasumori A. Porous properties of activated carbons from waste newspaper prepared by chemical and physical activation. Journal of Colloid and Interface Science. 2003 Jun;262(1):179–93.

37. Lua AC, Yang T. Effects of vacuum pyrolysis conditions on the characteristics of activated carbons derived from pistachio-nut shells. Journal of Colloid and Interface Science. 2004 Aug;276(2):364–72.

38. Ferrero F. Adsorption of Methylene Blue on magnesium silicate: Kinetics, equilibria and comparison with other adsorbents. Journal of Environmental Sciences. 2010 Jan;22(3):467–73.

39. Raposo F, De La Rubia MA, Borja R. Methylene blue number as useful indicator to evaluate the adsorptive capacity of granular activated carbon in batch mode: Influence of adsorbate/adsorbent mass ratio and particle size. Journal of Hazardous Materials. 2009 Jun 15;165(1–3):291–9.

40. Ma J, Yu F, Zhou L, Jin L, Yang M, Luan J, et al. Enhanced Adsorptive Removal of Methyl Orange and Methylene Blue from Aqueous Solution by Alkali-Activated Multiwalled Carbon Nanotubes. ACS Applied Materials & Interfaces. 2012 Nov 28;4(11):5749–60.